Geochimica et Cosmochimica Acta, Vol. 69, No. 8, pp. 2141–2151, 2005

0016-7037/05 $30.00 + .00

doi:10.1016/j.gca.2004.10.019

Conditions of core formation in the Earth: Constraints from Nickel and Cobalt partitioning

Nancy L. Chabot,[1,*] David S. Draper[2] and Carl B. Agee[2]

[1]Department of Geological Sciences, 112 A.W. Smith Bldg., Case Western Reserve University, Cleveland, OH, 44106-7216, USA.
[2]Institute of Meteoritics, Department of Earth and Planetary Sciences, University of New Mexico, Albuquerque, NM, 87131-1126 USA.

(*Received July* 12, 2004; *accepted in revised form October* 22, 2004)

Abstract—The abundances of Ni and Co in the Earth's mantle are depleted relative to chondrites due to terrestrial core formation. Recently, the observed mantle depletions of these elements have been explained by liquid metal-liquid silicate equilibrium during core formation in a high pressure, high temperature magma ocean on the early Earth. However, different magma ocean models, which would be expected to give consistent results, have proposed vastly different pressures (24 to 59 GPa), temperatures (2200 to >4000 K) and oxygen fugacities (−0.15 to −2.4 ΔIW) for the Earth's magma ocean. In an attempt to resolve the contradictory results from different magma ocean models and determine the thermodynamic conditions appropriate for core formation in the Earth, experiments were conducted to better constrain the influences of temperature and C on the partitioning behaviors of Ni and Co. Results of experiments at 7 GPa with temperatures of 1923–2673 K show that the metal-silicate partition coefficients for both Ni and Co decrease with increasing temperature, with the effect being more significant for Ni. Little change in the partitioning behaviors of either Ni or Co with varying C-content of the metallic liquid was found. By combining the new temperature data with previous results from pressure and oxygen fugacity studies, we parameterized the partitioning behavior of Ni and Co and applied the parameterizations to core formation in a terrestrial magma ocean. Multiple combinations of pressure, temperature, and oxygen fugacity can explain the observed mantle depletions of Ni and Co, and all of the very different previously proposed magma ocean conditions are generally consistent with valid solutions. By using the FeO content of the Earth's mantle as an additional constraint on the oxygen fugacity, magma ocean conditions of 30–60 GPa, > 2000 K, and −2.2 ΔIW are suggested. Similar systematic approaches and studies of other moderately siderophile elements could further constrain the magma ocean conditions on the early Earth.

1. INTRODUCTION

During core formation, due to their siderophile (metal-loving) nature, Ni and Co are strongly partitioned into the metallic core and become depleted in the Earth's mantle. One-atmosphere experimental partitioning results predict that Ni should be approximately an order of magnitude more depleted in the Earth's mantle than Co (e.g., review by Walter et al., 2000). In actuality, Ni and Co are similarly depleted in the Earth's mantle relative to their chondritic abundances; furthermore, both elements are overabundant in the Earth's mantle as compared to predictions from one-atmosphere experiments (Walter et al., 2000). Ringwood (1966) was the first to recognize the problem of the "excess" of Ni and Co, as well as other siderophile elements, in the Earth's mantle.

However, core formation in the Earth at high pressure and temperature, rather than at one atmosphere, could influence the partitioning behavior. Recent studies, based on high-pressure, high-temperature experimental data have identified core formation conditions under which the similar depletions of Ni and Co in the Earth's mantle can be explained (Li and Agee, 1996; Righter et al., 1997; Righter and Drake, 1999; Gessmann and Rubie, 2000; Li and Agee, 2001). All of these studies have proposed an early, deep, magma ocean on the Earth, out of which liquid metal segregated from molten silicate to eventually form the Earth's core.

Though the studies are all based on experimental partitioning data and all advocate a similar equilibrium, magma ocean core formation process, the different studies have proposed quite different magma ocean conditions for core formation in the Earth. The proposed pressure at the bottom of the magma ocean has ranged from 24 to 59 GPa, and the proposed temperature has varied from 2200 to >4000 K. There is also disagreement on the oxygen fugacity of the magma ocean, with proposed values ranging from 0.15 to 2.4 log units below the iron-wüstite buffer (−0.15 to −2.4 ΔIW). Additionally, Righter and Drake (2001) claimed that their work showed that Ni and Co could not be matched in the Earth's mantle using the higher pressures and temperatures proposed by Gessmann and Rubie (2000) and Li and Agee (2001). The studies of Li and Agee (1996); Righter et al. (1997); Righter and Drake (1999), and Li and Agee (2001) are all based on high-pressure, high-temperature metal-silicate partitioning experiments that were conducted using similar techniques. Studies based on similar experiments would be expected to produce consistent and similar results.

Furthermore, the specifics of the proposed magma ocean conditions have implications for other aspects of the Earth's evolution. For example, the pressure and temperature conditions proposed by Righter et al. (1997) and Righter and Drake (1999) are subsolidus when compared to a mantle peridotite phase diagram (Zhang and Herzberg, 1994), conditions which seem incompatible with core formation in a magma ocean.

* Author to whom correspondence should be addressed (Johns Hopkins Applied Physics Laboratory, 11100 Johns Hopkins Road, Laurel, MD 20723).

Righter et al. (1997) and Righter and Drake (1999) used this observation to argue that the early magma ocean must have been hydrous, which would depress the solidus temperature and allow the proposed magma ocean conditions to be consistent with molten silicate. The presence of an early hydrous magma ocean has potential implications for the initial volatile budget of the Earth. As another example, experimental studies have shown that the oxygen fugacity at the time when metal segregates from silicate will have an important influence on the non-metal content, such as the S, O, or Si-content, of the metal (Kilburn and Wood, 1997; Gessmann and Rubie, 1998; Hillgren et al., 2000). The specific conditions of core formation thus have implications for the identity of the light element(s) in the Earth's core.

Because of the importance of core formation and its implications for other aspects of the Earth's evolution, we have undertaken this study to determine the cause of the differing results from previous studies and to better constrain the conditions consistent with the mantle abundances of Ni and Co for core formation in a magma ocean. It should be noted that alternative hypotheses for core formation and the observed mantle abundances of siderophile elements in the Earth do exist (e.g., heterogenous accretion, Wänke, 1981). However, this study focuses on the partitioning behavior of Ni and Co during core formation in an early magma ocean. We begin by conducting experiments to better constrain the effects of temperature and C on the metal-silicate partitioning behaviors of Ni and Co. Preliminary results of this work were presented in Chabot and Agee (2002) and Chabot et al. (2004).

2. EXPERIMENTAL AND ANALYTICAL METHODS

All experiments were conducted using the University of New Mexico/Johnson Space Center multi-anvil at 7 GPa, using a castable octahedral assembly similar to that used by Agee et al. (1995). The castable octahedral assembly had a truncated edge length (TEL) of 8 mm. Furnaces of Re foil were used to heat the experiments, and the temperature was monitored using a W3Re/W25Re thermocouple. The thermocouple was positioned perpendicular to the axis of the cylindrical Re furnace and wrapped around the furnace. A dense alumina sleeve separated the Re furnace from the capsules. The starting silicate composition was natural Knippa basalt, a MgO-rich alkali olivine basalt (Lewis and Lofgren, 1991). The Knippa basalt has a lower melting point than a material such as a KLB-1 mantle peridotite, thus providing a larger possible range in experimental temperatures over which the silicate is molten. The starting metallic composition was Fe with about 10 wt% Ni, 4 wt% Co, and varying amounts of C, all added as commercially purchased powders. The amount of C was varied to examine the effect of C on D(Ni) and D(Co). Additionally, the presence of C in the Fe-Ni metal lowers the melting point (Okamoto, 1990; Wood, 1993), and consequently, the range of temperatures that can be experimentally covered while the metal remains a liquid is greater.

Experiments were run using alumina capsules, except for the most C-rich run, #Ni3, which was conducted in a graphite capsule. The alumina capsule reacted with the silicate melt, causing the final silicate melt to have elevated but homogeneous Al-contents relative to the starting Knippa basalt composition of 6.2 wt% Al (Lewis and Lofgren, 1991). Temperatures ranged from 1923 to 2673 K. Run durations varied inversely with temperature, ranging from 4 hours to 1.5 min. To achieve good separation of the metal and silicate phases, lower temperature runs #Ni20, #Ni24, and #Ni25 were first raised to 2273 K for 2 min and then lowered to their run temperatures. The choices of run durations were based on previous multi-anvil experimental studies that demonstrated that equilibrium was obtained during such run durations (Thibault and Walter, 1995; Gessmann and Rubie, 1998; Li and Agee, 2001; Chabot and Agee, 2003). The experiments #Ni20 and #Ni24, both conducted at 1973 K, gave consistent partitioning results despite the different run durations of 3 hours and 1 h respectively, suggesting that equilibrium was achieved in both runs. Table 1 and Table 2 list the experimental conditions of each run.

At run conditions, all experiments contained liquid metal and silicate melt. In the runs below 2073 K, garnet and spinel were also present, probably reflecting the lower temperature as well as the addition of Al from the capsule. Figure 1 shows some back scattered electron (BSE) images of a typical run product, run #Ni1. The metal and silicate form clearly distinguishable phases, though neither phase remains homogenous upon quenching. The silicate melt quench texture is composed of garnet quench crystals with interstitial material, as shown in Figure 1b. Silicate quench textures depended on the temperature and the composition, with a finer quench texture for the higher temperature runs, perhaps due to a combination of the destruction of nucleation sites and higher Al-content of the silicate. The quenched liquid metal, shown in Figure 1c, consisted of Fe-Ni dendrites surrounded by a C-rich metallic phase, with runs with similar C-contents having similar metallic quench textures, regardless of the run temperature.

Analysis was conducted using an electron microprobe, the NASA Johnson Space Center Cameca SX-100, the University of New Mexico JEOL 8200, or the Smithsonian Institution National Museum of Natural History JEOL JXA 8900R. Due to the quench textures, multiple analyses with a 20–50 μm defocused beam were used to determine the bulk compositions of the silicate melt and liquid metal at runs conditions. Major elements were analyzed using beam conditions of 15 kV and 20–50 nA with counting times of 20 s. Concentrations as low as 300 ppm of Ni and Co in the silicate were measured with a beam of 15 kV and 50–200nA and by counting for 60–120 s. Errors were calculated as twice the standard deviation of the mean. Oxygen was measured in some of the metals, but due to the lack of appropriate standards, the measurements have a significant uncertainty and consequently are reported to only one significant figure. The O concentrations in the silicate were calculated based on standard valences for the measured major elements (4+ Si, Ti; 3+ Al; 2+ Fe, Mg, Ca; 1+ Na, K).

Analyzing C using the electron microprobe is an involved task, due to the difficulty of obtaining reliable standards, the C-coat on the sample, and the contamination of the sample from C within the probe itself (e.g., Wood, 1993). Thus, the C-content of the metallic liquid was not measured in the runs but rather was calculated as the difference of the metal total from 100%. During the analysis of each new run product, the metal of #Ni2, the C-free experiment, was also re-analyzed to be sure that its total was still 100% within error. The uncertainty in the calculated C-content is thus taken to be the uncertainty of the total, which is about 1.5 wt%. The C-content deduced by this method for run #Ni3, which was conducted in a graphite capsule, is generally consistent with the C-content expected from the calculated Fe-C phase diagrams at 5–15 GPa (Wood, 1993). As will be discussed in the following section, the effect of C on D(Ni) and D(Co) is small, and thus estimating the C-content of our experiments does not affect any of the core formation implications of this work.

3. EXPERIMENTAL RESULTS

In this study, the partition coefficient (D) is defined as the weight concentration of an element in the liquid metal divided by the weight concentration of the same element in the liquid silicate. To compare experiments and to determine the effects of thermodynamic variables other than oxygen fugacity, it is necessary to normalize all of the experiments to a common oxygen fugacity. Experiments conducted at 1 atm have shown that Ni and Co behave as divalent species in the silicate melt over a wide range of oxygen fugacities (Capobianco and Amelin, 1994; Dingwell et al., 1994; Holzheid et al., 1994). Using a valence of 2+, the effect of oxygen fugacity on the metal-silicate partitioning of Ni and Co can be quantified as:

$$\log[D] \propto -0.5(\triangle \mathrm{IW}) \quad (1)$$

where D is the partition coefficient, ΔIW is the difference in

Table 1. Experimental run conditions and analytical results for systematic study of effect from C.

Run #	Ni2	Ni4	Ni5	Ni1	Ni3
Pressure (GPa)	7	7	7	7	7
Temp. (K)	2273	2273	2273	2273	2273
Duration (min)	6	6	6	6	6
Metal (wt %)					
Fe	86.8 ± 0.2	81.6 ± 0.2	85.0 ± 0.2	84.8 ± 0.2	84.5 ± 0.1
Ni	10.1 ± 0.1	12.5 ± 0.1	8.0 ± 0.1	6.7 ± 0.1	6.4 ± 0.1
Co	2.7 ± 0.1	4.4 ± 0.1	4.1 ± 0.1	4.4 ± 0.1	2.4 ± 0.1
O	0.4	0.3	0.4	0.6	0.3
Total	100.0	98.8	97.5	96.5	93.6
C*	0	1.2	2.5	3.5	6.4
Silicate (wt %)					
Si	16.3 ± 0.1	15.8 ± 0.2	12.1 ± 0.5	15.6 ± 0.2	18.4 ± 0.1
Ti	1.3 ± 0.1	1.3 ± 0.1	1.0 ± 0.1	1.4 ± 0.1	1.7 ± 0.1
Al	13.6 ± 0.6	14.7 ± 0.6	22.6 ± 1.3	13.7 ± 0.3	6.6 ± 0.1
Fe	12.5 ± 0.4	12.0 ± 0.3	10.6 ± 0.4	11.3 ± 0.2	12.5 ± 0.2
Mg	4.9 ± 0.1	5.4 ± 0.1	3.8 ± 0.2	5.7 ± 0.1	8.2 ± 0.2
Ca	6.7 ± 0.1	6.2 ± 0.1	4.9 ± 0.2	7.1 ± 0.1	7.4 ± 0.1
Na	1.6 ± 0.1	1.4 ± 0.1	1.4 ± 0.1	1.4 ± 0.1	1.5 ± 0.1
K	1.3 ± 0.1	1.2 ± 0.1	1.2 ± 0.1	1.0 ± 0.1	1.6 ± 0.1
Ni	0.039 ± 0.004	0.056 ± 0.006	0.031 ± 0.006	0.029 ± 0.004	0.036 ± 0.005
Co	0.029 ± 0.004	0.066 ± 0.004	0.046 ± 0.006	0.059 ± 0.004	0.037 ± 0.004
O#	42.0	42.3	42.8	41.4	40.7
Total	100.3	100.4	100.5	98.7	98.7
Calculated					
log fO_2-log IW	−1.53	−1.48	−1.51	−1.48	−1.39
D(Ni)	260 ± 30	220 ± 20	260 ± 50	230 ± 30	180 ± 30
D(Co)	93 ± 13	67 ± 4	89 ± 12	75 ± 5	65 ± 8

Errors are ± 2 standard deviations of the mean. Experiments were run in alumina capsules, except for #Ni3 which was run in graphite.
* Carbon content calculated as the difference of the metal total from 100%.
# Oxygen content calculated based on the following valences of the major elements in the silicate: +4 Si, Ti; +3 Al; +2 Fe, Mg, Ca; +1 Na, K.

oxygen fugacity defined in log units relative to the iron-wüstite buffer, and the value of 0.5 arises because Ni and Co are taken to be divalent. The oxygen fugacity is not measured during each experiment but rather is estimated using the resulting metallic and silicate compositions. Hillgren et al. (1994) estimated ΔIW as:

$$\Delta IW = 2 \log (a_{FeO}/a_{Fe}) \quad (2)$$

with a_{FeO} as the activity of FeO in the silicate melt and a_{Fe} as the activity of Fe in the liquid metal. The estimated oxygen fugacity is thus based completely on the partitioning behavior of Fe. If the metal is pure Fe, $a_{Fe} = 1$. Otherwise, the atomic concentration of Fe in the metal is used as an estimate for a_{Fe}. By assuming ideal behavior, the value of a_{FeO} is crudely estimated as the molar FeO concentration of the silicate. Asahara et al. (2004) have shown that estimates of the oxygen fugacity using Eqn. 2 that were based on the FeO-content of the silicate melt were about 0.3 log units lower than oxygen fugacity estimates determined using the FeO-content of coexisting magnesiowüstite. For consistency, we calculated all of the estimates of oxygen fugacity, of our experiments and of previous studies, using the FeO-content of the silicate melt.

Figure 2 plots D(Ni) and D(Co) from experiments conducted at 2273 K as a function of the C-content of the metal, normalized to an oxygen fugacity of −1.5 ΔIW. The experimental results are tabulated in Table 1. The effect of C, a potential light element in the Earth's core (Wood, 1993), on D(Ni) and D(Co) is small, and there is no evidence for fundamentally different partitioning behaviors in the C-free and graphite saturated systems. Once normalized to a common oxygen fugacity, a comparison of the C-free run #Ni2 with the graphite-saturated run #Ni3 shows a decrease of about 20% in both D(Ni) and D(Co) due to the presence of about 6.4 wt% C. These observed decreases in D(Ni) and D(Co) are consistent with the previous results from the C-free and graphite-saturated experiments of Jana and Walker (1997a) and the solid metal-liquid metal C-bearing partitioning work for Ni of Lauer and Jones (1999).

These results indicate that experiments can be compared over a wide range of C-contents, from C-free to graphite-saturated. Jones (1998) criticized the study of Righter et al. (1997) for including both C-bearing and C-free experiments in their core formation models without accounting for the effect of C. Subsequently, Righter and Drake (1999) included a variable for the effect of C and obtained different parameterization values for Ni and Co than in their previous work. One could think the change was due to including the effect of C, but our new results indicate the effect of C on D(Ni) and D(Co) is small. Our results show that the effect of C on D(Ni) and D(Co) can be treated as negligible in core formation models.

The experimentally determined effects of temperature on D(Ni) and D(Co) are shown in Figure 3, with all runs normalized to an oxygen fugacity of −1.5 ΔIW. Table 2 lists the results of runs that were conducted to determine the effect of temperature. However, all experiments from both Tables 1 and 2 are shown on Figure 3, since varying C-contents have little effect on D(Ni) and D(Co). At 7 GPa, both D(Ni) and D(Co) decrease with increasing temperature, though the effect is more pronounced for Ni than for Co.

Table 2. Experimental run conditions and analytical results for systematic study of the effect of temperature.

Run #	Ni25	Ni20	Ni24	Ni10	Ni18	Ni8	Ni19	Ni21	Ni22
Pressure (GPa)	7	7	7	7	7	7	7	7	7
Temp. (K)	1923	1973	1973	2073	2173	2373	2473	2573	2673
Duration (min)	240	180	60	90	30	4	3	3	1.5
Metal (wt %)									
Fe	82.4 ± 0.3	80.4 ± 0.2	83.5 ± 0.1	83.2 ± 0.2	81.3 ± 0.3	84.4 ± 0.3	81.9 ± 0.2	81.4 ± 0.2	81.1 ± 0.6
Ni	11.7 ± 0.2	13.2 ± 0.2	10.2 ± 0.1	10.7 ± 0.1	12.3 ± 0.3	7.2 ± 0.1	12.0 ± 0.2	12.5 ± 0.1	12.1 ± 0.2
Co	4.1 ± 0.1	4.1 ± 0.1	4.0 ± 0.1	3.8 ± 0.1	4.1 ± 0.1	3.7 ± 0.1	3.9 ± 0.1	4.1 ± 0.1	3.9 ± 0.1
O	n.a.	n.a.	n.a.	0.6	n.a.	0.3	n.a.	n.a.	n.a.
Total	98.2	97.7	97.7	98.3	97.7	95.6	97.8	98.0	97.1
C*	1.8	2.3	2.3	1.7	2.3	4.4	2.2	2.0	2.9
Silicate (wt %)									
Si	15.9 ± 0.1	17.4 ± 0.1	16.0 ± 0.1	15.1 ± 0.4	16.2 ± 0.1	14.4 ± 0.4	14.6 ± 0.5	12.8 ± 0.2	10.8 ± 0.3
Ti	2.6 ± 0.1	1.8 ± 0.1	1.9 ± 0.1	1.4 ± 0.1	1.4 ± 0.1	1.1 ± 0.1	1.2 ± 0.1	1.0 ± 0.1	0.7 ± 0.1
Al	6.6 ± 0.1	8.6 ± 0.3	7.6 ± 0.1	11.0 ± 0.8	11.5 ± 0.1	17.8 ± 0.9	16.9 ± 1.5	21.7 ± 0.8	26.6 ± 1.0
Fe	15.3 ± 0.1	15.4 ± 0.1	18.0 ± 0.1	17.3 ± 0.6	14.4 ± 0.2	11.2 ± 0.3	12.4 ± 0.5	11.7 ± 0.4	9.5 ± 0.5
Mg	1.6 ± 0.1	2.4 ± 0.1	2.6 ± 0.1	3.9 ± 0.2	4.6 ± 0.1	4.7 ± 0.1	4.4 ± 0.2	3.7 ± 0.1	4.9 ± 0.2
Ca	2.9 ± 0.1	4.9 ± 0.1	5.3 ± 0.1	6.8 ± 0.3	6.8 ± 0.1	5.9 ± 0.2	6.2 ± 0.3	5.4 ± 0.1	3.8 ± 0.1
Na	9.4 ± 0.1	5.6 ± 0.3	5.8 ± 0.1	2.6 ± 0.3	1.7 ± 0.1	1.3 ± 0.1	1.2 ± 0.1	1.1 ± 0.1	0.9 ± 0.1
K	7.4 ± 0.1	4.7 ± 0.1	4.5 ± 0.1	1.1 ± 0.1	1.3 ± 0.1	0.8 ± 0.1	0.9 ± 0.1	0.7 ± 0.1	0.6 ± 0.1
Ni	b.d.	0.040 ± 0.008	0.031 ± 0.006	0.061 ± 0.008	0.039 ± 0.003	0.043 ± 0.006	0.053 ± 0.002	0.064 ± 0.008	0.069 ± 0.006
Co	0.059 ± 0.003	0.073 ± 0.011	0.085 ± 0.006	0.062 ± 0.006	0.077 ± 0.002	0.059 ± 0.006	0.076 ± 0.006	0.086 ± 0.005	0.073 ± 0.005
O#	37.1	39.5	38.2	39.3	40.4	42.4	42.0	43.0	44.3
Total	98.9	100.4	100.0	98.6	98.4	99.7	99.9	101.3	102.2
Calculated									
log fO_2-log IW	−1.23	−1.21	−1.11	−1.14	−1.28	−1.44	−1.40	−1.42	−1.56
D(Ni)	b.d.	330 ± 70	330 ± 60	180 ± 20	320 ± 30	170 ± 20	230 ± 10	200 ± 30	180 ± 20
D(Co)	70 ± 4	56 ± 9	47 ± 4	61 ± 6	53 ± 2	63 ± 7	51 ± 4	48 ± 3	53 ± 4

Errors are ± 2 standard deviations of the mean. All experiments were in alumina capsules.
n.a. Not Analyzed.
b.d. Below Detection limits.
* Carbon content calculated as the difference of the metal total from 100%.
# Oxygen content calculated based on the following valences of the major elements in the silicate: +4 Si, Ti; +3 Al; +2 Fe, Mg, Ca; +1 Na, K.

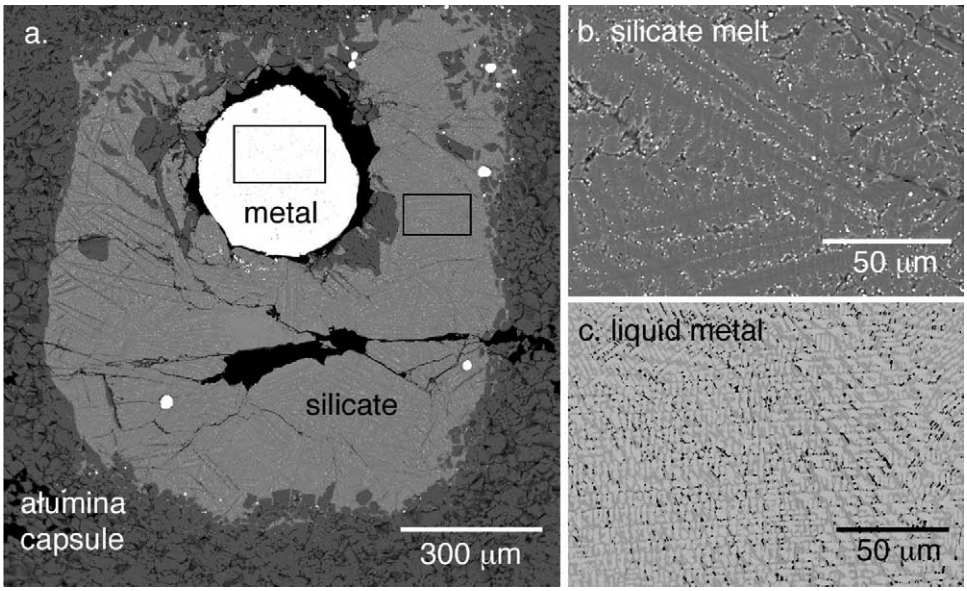

Fig. 1. Back scattered electron images of #Ni1 show the characteristic form and textures of a typical run product. **a.** The run is contained in an alumina capsule (dark gray), pieces of which can also be seen near the edge of the metal and in the silicate. The metal (white) and silicate (light gray) form well-separated phases, each of which was homogenous at run conditions. Black areas around the metal and in the silicate are epoxy-filled voids. **b.** The silicate melt quenches to a combination of garnet crystals (dark gray) and interstitial material. **c.** The C-bearing metallic liquid quenches to Fe-Ni dendrites, which are the brighter phase in the image, surrounded by C-rich material.

The observed decrease in D(Ni) and D(Co) with increasing temperature is generally consistent with the previous one-atmosphere studies of Capobianco and Amelin (1994) and Holzheid and Palme (1996), which each covered a temperature range of <300 K. At pressures above one-atmosphere, Thibault and Walter (1995) conducted experiments at 5 GPa and three different temperatures, over a total range of 450 K; Li and Agee (2001) also ran experiments at three different temperatures, with a smaller overall range of 350 K, at 10 GPa. Though limited to essentially three points and a small range in temperature to constrain the slopes, both of these studies suggested some decrease in D(Ni) and D(Co) with increasing temperature, consistent with our new result in Figure 3. Additional temperature data in Agee et al. (1995) and Li and Agee (2001) (C-bearing experiments) were also examined, but the S-contents in the metallic liquid of these studies have ranges too large to make the data sets useful for determining the effect of temperature.

With the effect of temperature now better characterized for D(Ni) and D(Co), we can compare our experimental results to the temperature effect predicted by different magma ocean models. Figure 4 illustrates the severity of the different predicted effects of temperature on D(Ni) and D(Co) of the previous models. In Figure 4, which was calculated for a pressure of 7 GPa, all models are defined to have the same D at 1900 K, but by 4500 K, the D predicted by the models can differ by over an order of magnitude. The studies of Righter et al. (1997) and Righter and Drake (1999) use a large number of experiments, >200, in their parameterizations of D(Ni) and D(Co). However, the number of experiments is not nearly as important as the range of experimental conditions spanned. The large majority of the >200 experiments used in their parameterizations are at 1 atm and low temperatures. The lack of high temperature data might explain the surprising change in the temperature predictions between the work of Righter et al. (1997) and Righter and Drake (1999), shown on Figure 4. The model of Li

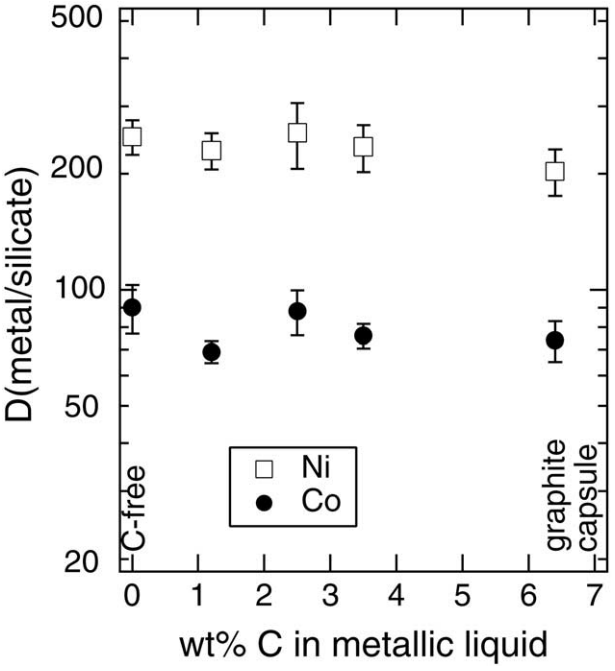

Fig. 2. Experiments conducted at 2273 K and 7 GPa are plotted as a function of the C-content of the metallic liquid, with runs normalized to −1.5 ΔIW. Carbon has little effect on D(Ni) or D(Co), even when experiments are conducted at the two extreme end-member conditions of C-free and graphite-saturated. Error bars are ± 2σ.

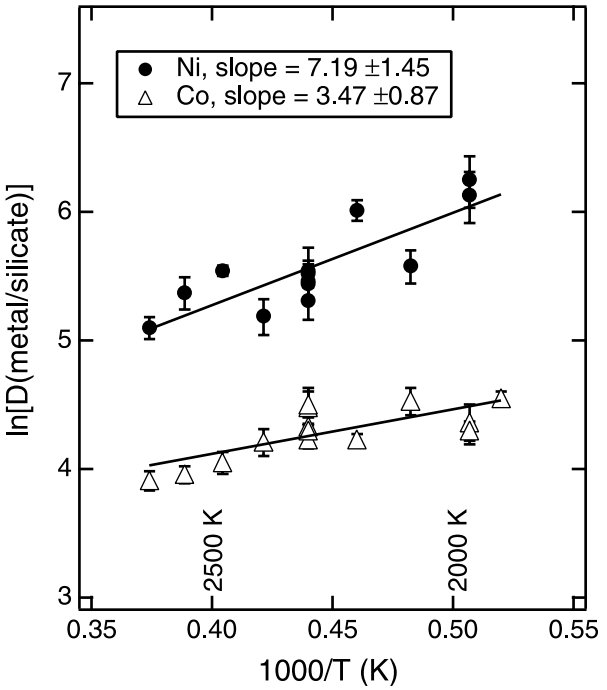

Fig. 3. All of the experiments from Tables 2 and 3 are plotted as a function of the run temperature. Experiments were conducted at 7 GPa and have been normalized to an oxygen fugacity of −1.5 ΔIW. Runs have varying C-contents in the metallic liquid, but as Figure 2 shows, this has little effect on the partitioning behavior. Both D(Ni) and D(Co) decrease with increasing temperature, though the change with temperature is greater for D(Ni). Best-fit lines are used to parameterize the data, and error bars are ± 2σ.

and Agee (2001) is based only on their own experimental work and uses 15 experiments to constrain 6 variables. The experimental temperature data used in their model come from 3 experiments that vary by 350 K and are likely not adequate to effectively constrain the effect of temperature. In contrast to the other models, the work of Gessmann and Rubie (2000) is based on liquid metal-magnesiowüstite partitioning data. However, it has been shown that liquid metal-magnesiowüstite partition coefficients can differ slightly from liquid metal-liquid silicate values and consequently metal-magnesiowüstite partition coefficients may not be a good proxy for the liquid silicate-liquid metal partitioning that occurred in an early magma ocean (Chabot and Agee, 2003).

Figure 4 shows how our data and best-fit lines compare to the previous model predictions. For D(Ni), our best-fit line is intermediate to the predictions of Righter et al. (1997) and Li and Agee (2001), the two models which predict the largest effect of temperature at 7 GPa. For D(Co), our data fall in between the predictions of Gessmann and Rubie (2000); Righter et al. (1997), and Li and Agee (2001). The predicted increase in D(Co) with increasing temperature of Righter and Drake (1999) is inconsistent with our temperature data set.

4. PARAMETERIZING D(NI) AND D(CO)

To model core formation, we need to express D(Ni) and D(Co) as a function of the thermodynamic variables that affect their partitioning behaviors. Our new experimental results better constrain the effect of temperature on D(Ni) and D(Co) and also indicate that the effect of C in the metallic liquid can be safely neglected during our modeling. The effect of oxygen fugacity on D(Ni) and D(Co) is taken from previous work that has demonstrated that Ni and Co behave as divalent species, as already discussed for Eqn. 1 (Capobianco and Amelin, 1994; Dingwell et al., 1994; Holzheid et al., 1994). However, other variables, such as other metallic compositions, silicate compo-

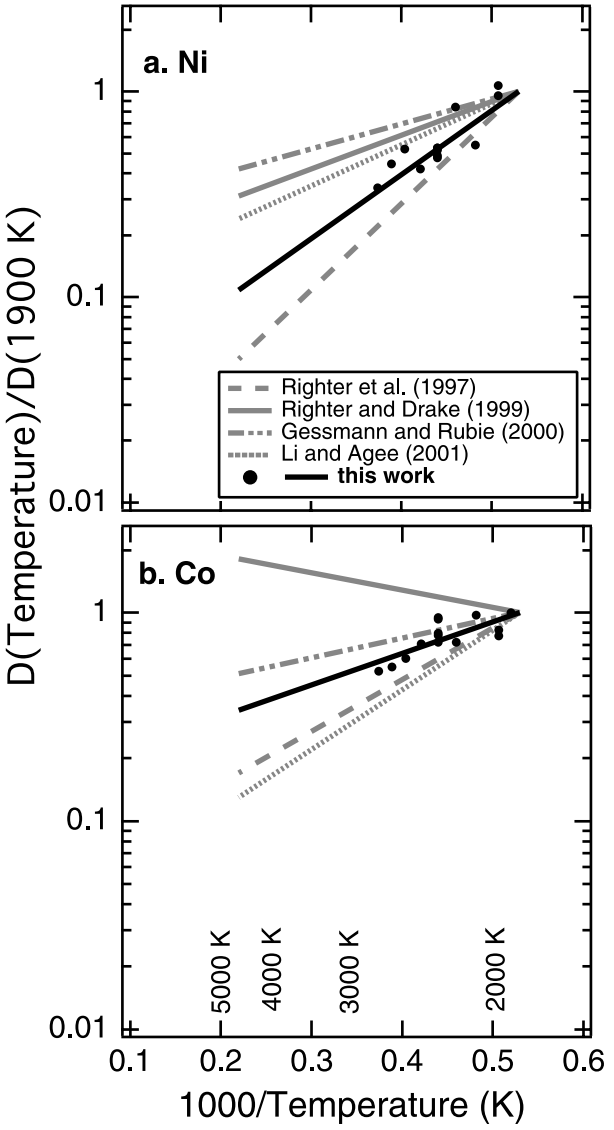

Fig. 4. The predicted behaviors of **a.** D(Ni) and **b.** D(Co) from different core formation models as a function of temperature and at 7 GPa are compared to our experimental data. For comparison, the ratio of the partition coefficient relative to its value at 1900 K is shown, and thus at a temperature of 1900 K, the ratio is defined as 1 for all of the models. The different predicted effects of temperature by the different models contributed significantly to the discrepancies between the different proposed conditions of core formation. Our experimental temperature data for D(Ni) suggest a temperature effect intermediate to the effects predicted by Righter et al. (1997) and Li and Agee (2001). For D(Co), our data suggest a temperature effect intermediate to the proposed effects of Gessmann and Rubie (2000) and Righter et al. (1997). The predicted increase in D(Co) with increasing temperature of Righter and Drake (1999) is inconsistent with our new experimental data.

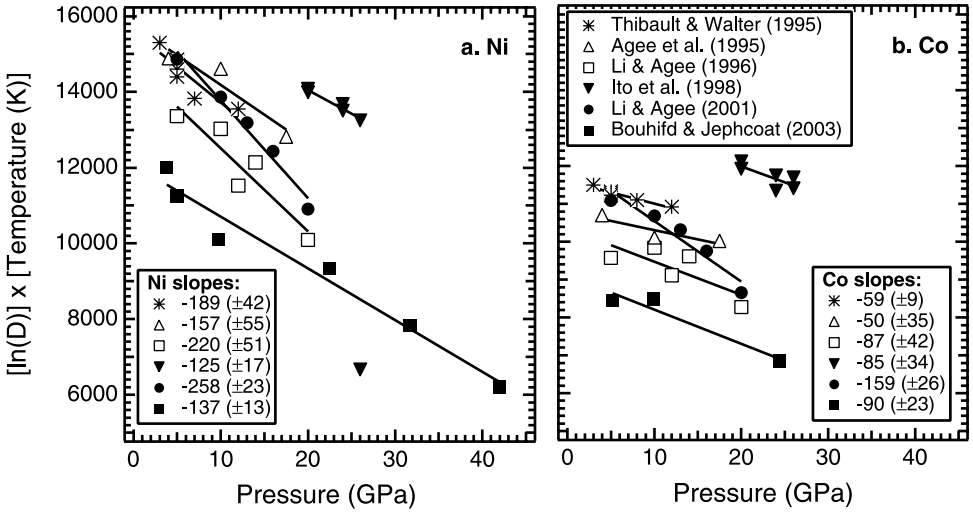

Fig. 5. Previous experimental partitioning studies of **a.** Ni and **b.** Co in which temperature and composition were held constant for each study are normalized to an oxygen fugacity of −1.5 ΔIW and plotted as a function of pressure. The slopes from each study are expected to be the same when plotted in this form of ln(D)*Temperature vs. Pressure. Weighted averages and uncertainties yield best estimates for the Ni slope of −157 ± 9 and for the Co slope of −72 ± 8. The temperatures of the experimental studies were: Thibault and Walter (1995), 2500 K; Agee et al. (1995), 2273 K; Li and Agee (1996), 2273 K; Ito et al. (1998), 2873 K; Li and Agee (2001), 2273 K; Bouhifd and Jephcoat (2003), 2500 K.

sition, and pressure, can influence metal-silicate partitioning behavior and need to be considered when parameterizing D(Ni) and D(Co).

Results of solid metal-liquid metal partitioning experiments have shown that the S-content of the metallic liquid can have a large effect on the partitioning behavior; however, for siderophile elements, the effect of S is most pronounced at high S-contents (S >20 wt%) (Jones and Drake, 1983). For Ni and Co, in the range of S-contents applicable to the Earth's core, most recently estimated to be ≤7.3 wt% S (Anderson and Isaak, 2002), the solid metal-liquid metal partitioning behavior varies by less than a factor of 1.3 (Chabot and Jones, 2003). Additionally, Jana and Walker (1997c) determined that the effect of S on Ni and Co metal-silicate partitioning behavior is consistent with the solid metal-liquid metal experiments. Thus, the effect of S on the partitioning of Ni and Co is minor over the range of S-contents pertinent to core formation in the Earth and consequently can be neglected. Effects from other potential light elements, such as H, O, and Si, are also assumed to be negligible in this work, though more data are needed to either support or disprove this assumption.

Experimental studies have suggested that the influence of silicate melt composition on D(Ni) and D(Co) is also minor in the pressure and temperature regime of this work, and the previous studies have attributed this lack of influence to the 2+ valences of the elements (e.g., Jana and Walker, 1997b; Jaeger and Drake, 2000). In our modeling, we make the assumption that any effect from silicate composition can be neglected for Ni and Co. Later in this section, when we apply the parameterized expressions for D(Ni) and D(Co) to the experimental data of this and other studies, the success of the parameterizations to match experiments with different silicate compositions without a silicate composition term provides additional support for the validity of treating silicate compositional effects as negligible for D(Ni) and D(Co).

Multiple experimental studies have demonstrated that both D(Ni) and D(Co) decrease with increasing pressure, and these previous studies, each of which held temperature and composition constant while varying pressure, are shown on Figure 5 (Agee et al., 1995; Thibault and Walter, 1995; Li and Agee, 1996; Ito et al., 1998; Li and Agee, 2001; Bouhifd and Jephcoat, 2003). The data on Figure 5 have been normalized to an oxygen fugacity of ΔIW = −1.5. The scales on Figure 5 were chosen because, by thermodynamic relations, ln(D) should be linearly related to the term P/T (pressure divided by temperature), and thus, all six of the studies plotted on Figure 5 should exhibit the same slope on such a plot. Additionally, only experiments conducted at pressures ≥3 GPa were included on Figure 5, since recent work suggests that the effect of pressure is more extreme at lower (< 3 GPa) pressures than at higher pressures (Kegler et al., 2004). In this study, we are interested in applying the results to the conditions of core formation in an early terrestrial magma ocean, which involves pressures much greater than 3 GPa.

In general, there is good agreement between the different D(Ni) and D(Co) studies, given the scatter in the experimental data and the limited pressure range of some studies; all studies show a decrease in D(Ni) and D(Co) with increasing pressure, with the decrease being steeper for D(Ni) than for D(Co). One experimental D(Ni) point from Ito et al. (1998) is clearly inconsistent with the rest of the data. A close examination of Table 3 of Ito et al. (1998) suggests that the inconsistency is likely due to a typographical error in the reported NiO content of the silicate; in their Table 3, the reported ratio between the partitioning of Fe and Ni is consistent with the other data and cannot be produced using the reported NiO content of the silicate melt. Taking the six slopes and their uncertainties for D(Ni) and D(Co) from Figure 5, we calculate a weighted average and weighted one standard deviation uncertainty of −157 ± 9 and −72 ± 8 respectively.

Table 3. Parameters from core formation models.

Reference	C_1	C_2	C_3
Ni			
Righter et al. (1997)	11112	−222	0.57
Righter and Drake (1999)	5387	−231	4.1
Gessmann and Rubie (2000)*	3817	−153	1.8
Li and Agee (2001)	5890	−187	3.1
THIS WORK	8290 (± 1450)	−157 (± 9)	0.42 (± 0.05)
Co			
Righter et al. (1997)	6340	−104	0.89
Righter and Drake (1999)	−1213	−101	5.3
Gessmann and Rubie (2000)*	2691	−77	0.4
Li and Agee (2001)	7014	−69	0.25
THIS WORK	3920 (± 870)	−72 (± 8)	0.76 (± 0.05)

Parameterization form: $\ln(D) = C_1[I/T(K)] + C_2[P(GPa)/T(K)] - 0.5*\ln(10)*\Delta IW + C_3$

* The Gessmann and Rubie (2000) study was based on metal-magnesiowustite partitioning data while all other studies were based on metal-silicate experiments.

To parameterize the partition coefficients, we use a mathematical expression with pressure, temperature, and oxygen fugacity terms based on thermodynamic relations. The form of the parameterization for Ni and Co is:

$$\ln(D) = C_1[1/T] + C_2[P/T] - 0.5 * \ln(10) * \Delta IW + C_3 \quad (3)$$

where the temperature is expressed in Kelvin and the pressure is expressed in GPa. The constants C_1, C_2, and C_3 are specific to the partitioning behaviors of Ni and Co. The oxygen fugacity term assumes a 2+ valence for Ni and Co, as previously discussed. Equation 3 is the same form used by the models of Gessmann and Rubie (2000) and Li and Agee (2001), except for the use of a base 10 logarithm rather than a natural logarithm by Li and Agee (2001) and the elimination of the effect of oxygen fugacity as a fitted parameter. The parameterizations of Righter et al. (1997) and Righter and Drake (1999) differ from Eqn. 3 in the use of an absolute oxygen fugacity instead of an oxygen fugacity relative to the iron-wüstite buffer. However, it is easy to show that the two forms are mathematically equivalent but simply represent a different grouping of the pressure, temperature, and oxygen fugacity terms. In addition to the pressure, temperature, and oxygen fugacity dependencies, terms are commonly added to Eqn. 3 to take into account effects of the silicate and metal compositions, but, as discussed, such terms can be neglected for D(Ni) and D(Co) in the pressure and temperature range relevant to the present discussion.

Our experimental data were used to determine the effect of temperature. The slope of the best-fit line shown on Figure 3 represents the quantity $[C_1 + C_2(P)]$ from Eqn. 3; using our experimental pressure of 7 GPa and the weighted averages of C_2 calculated from the pressure studies on Figure 5, the value of C_1 for both D(Ni) and D(Co), and the associated error, were calculated. The last constant, C_3, was calculated by averaging the values of C_3 determined by each of our experiments as well as from all of the appropriate experiments of previous studies (Hillgren et al., 1994, 1996; Thibault and Walter, 1995; Ohtani et al., 1997; Righter et al., 1997; Jana and Walker, 1997a, 1997c; Ito et al., 1998; Gessmann and Rubie, 1998; Bouhifd and Jephcoat, 2003). By including all available experimental data, any minor effects from differences in silicate and metallic compositions or any systematic error in a given data set were minimized in the final parameterizations. Previous experiments with >10 wt% S in the metallic liquid were not included because at higher S-contents, the effect of S on D(Ni) and D(Co) increases and can not be neglected (Chabot et al., 2003). As discussed, only experiments run at ≥3 GPa were included and, according to the work of Kegler et al. (2004), our parameterizations may not be appropriate for use at lower pressures. Experiments at any temperature, oxygen fugacity, and with any C-content were included. For consistency, the oxygen fugacities for all previous experiments were computed relative to the iron-wüstite buffer using the method detailed in Eqn. 2.

As shown in Figure 6, the predicted partition coefficients from the parameterizations are generally within a factor of two of the measured values. The only notable exception is the work of Righter et al. (1997), where the predicted values for both D(Ni) and D(Co) are much higher than the measured values. Although the source of the discrepancy is unknown, we note that there are only two >3 GPa experiments reported in the Righter et al. (1997) paper and that the durations for the experiments were only a few minutes: 3 min. at 2023 K, 7 GPa, and 7 min. at 1923 K, 7 GPa. In comparison, our experiment #Ni25, also conducted at 1923 K and 7 GPa, was run for a duration of 4 hours. Thus, the two experiments of Righter et al. (1997) were excluded from the final calculation of C_3, and the uncertainty in C_3 was calculated as the standard deviation of the mean. Table 3 lists the constants C_1, C_2, and C_3 from Eqn. 3 determined by this work and used by previous core formation models for D(Ni) and D(Co).

The fact that the large majority of all available and appropriate experiments are fit within a factor of two on Figure 6 demonstrates the robustness of the parameterizations, in the pressure (3–42 GPa) and temperature (1923–2873 K) regimes that have been studied, and also their limitations. Judging from the errors given on the constants C_1, C_2, and C_3 in Table 3, the largest contributor to the uncertainties of the parameterizations comes from our determination of the effect of temperature on D(Ni) and D(Co). Taking the derivative of Eqn. 3 and assuming the errors are independent, we determined an expression for the uncertainty in the ln(D) that was a function of pressure and temperature. In the pressure and temperature ranges suggested

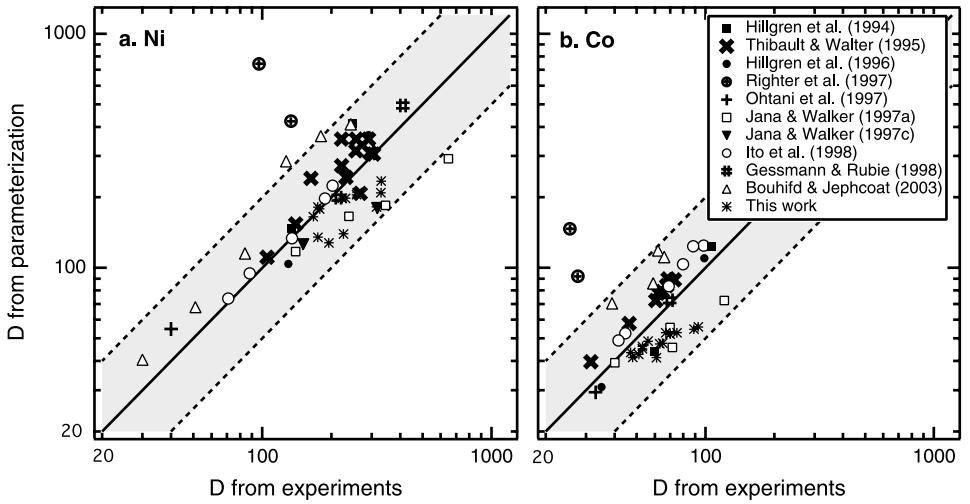

Fig. 6. All previously published determinations of **a.** D(Ni) and **b.** D(Co) from experiments conducted at ≥3 GPa and with <10 wt% S in the metallic liquid are compared to the partitioning values predicted from our parameterizations. With the exception of the two experiments from Righter et al. (1997), the experimental data are generally well matched by the parameterizations within a factor of two, shown by the shaded regions.

by previous magma ocean models, the resulting uncertainties in ln(D(Ni)) varied from 0.40–0.73, which is a factor of 1.5–2.1 uncertainty in D(Ni). For D(Co), the uncertainty was lower, within a factor of 1.3–1.6. These uncertainty determinations are in general agreement with the observation that the experimental data are well fit within a factor of two by the parameterized expressions.

5. MODELING CORE FORMATION

With our two equations for D(Ni) and D(Co), we can not uniquely constrain the three variables of pressure, temperature, and oxygen fugacity. However, we can examine the possible pressure and temperature solutions at the different proposed oxygen fugacity conditions. As shown, our parameterizations for D(Ni) and D(Co) seem to be accurate to within a factor of two. Thus, a given pressure and temperature combination is considered a solution if both D(Ni) and D(Co) from the parameterizations fall within a factor of two of the partitioning values needed to match the observed mantle depletions, which are about 25–28 for D(Ni) and 23–25 for D(Co) (McDonough and Sun, 1995).

Figure 7 illustrates the pressure and temperature solution spaces for the two different oxygen fugacities that have been proposed for an early terrestrial magma ocean. The studies of Righter et al. (1997) and Righter and Drake (1999) advocated conditions of −0.15 to −0.4 ΔIW, ~27 GPa, and ~2250 K; this pressure-temperature combination is slightly higher than our determined solution space at that oxygen fugacity but does overlap with our solution space within the errors given by Righter and Drake (1999). At a lower oxygen fugacity of ~ −2.2 ΔIW, as proposed by Gessmann and Rubie (2000) and Li and Agee (2001), the solution space encompasses combinations of higher pressures and temperatures, also consistent with the conditions suggested by these two studies. Thus, we find that all of the pressure, temperature, and oxygen fugacity combinations proposed by previous core formation models are

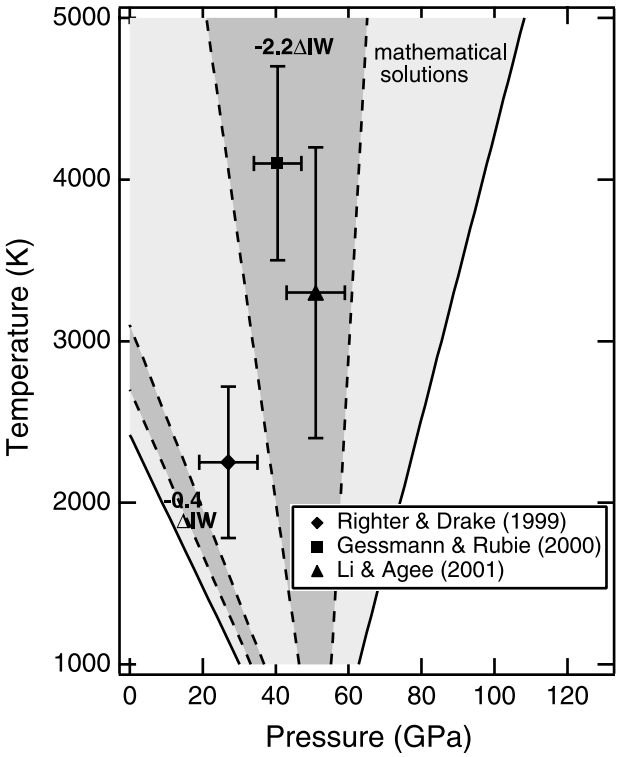

Fig. 7. Pressure and temperature solutions for two different oxygen fugacities are specifically shown as dark shaded regions, while the larger, lighter shaded region illustrates all of the possible mathematical solutions at any oxygen fugacity. A solution is defined as when the D(Ni) and D(Co) determined from our parameterizations fall within a factor of two of the partitioning values required to explain the observed mantle depletions. Based on only those criteria, for the pressure and temperature range shown, there are mathematical solutions at oxygen fugacities ranging from 0 to −3.4 ΔIW. At −0.4 ΔIW and −2.2 ΔIW, the two oxygen fugacities that have been proposed by previous core formation models, the pressure and temperature combinations advocated by previous studies (Righter et al., 1997; Righter and Drake, 1999; Gessmann and Rubie, 2000; Li and Agee, 2001) are all roughly consistent within error of our newly determined solution spaces.

generally mathematically possible, despite the wide range in proposed conditions. The success of all previous models does disprove the claim of Righter and Drake (2001) that the mantle abundance of Co cannot be matched by partitioning at the higher pressure, higher temperature, and lower oxygen fugacity conditions that have been proposed; our results demonstrate that Co can indeed be matched at these conditions.

In addition to the two solution spaces specifically shown on Figure 7, for other oxygen fugacities, there are also other pressure and temperature combinations that yield mathematical solutions. For the pressure and temperature ranges shown on Figure 7, mathematical solutions exist for oxygen fugacities from 0 to −3.4 ΔIW, as illustrated by the lighter shaded region on Figure 7. Not all of the mathematical solutions are physically plausible, such as solutions with combinations involving high pressure and low temperature. However, the existence of multiple solutions weakens the argument of Righter et al. (1997) and Righter and Drake (1999) that the early magma ocean must have been hydrous. Their interpretation was based on their proposed pressure and temperature solution falling below the dry mantle peridotite solidus (Zhang and Herzberg, 1994); thus, a depression of the solidus temperature due to the presence of water was suggested to have a liquid silicate phase stable, as would be required in a magma ocean. However, our work shows that there are multiple pressure and temperature solutions, many of which are above the dry mantle peridotite solidus and don't require an early terrestrial magma ocean to be hydrous.

To distinguish between our many solutions, additional constraints are required. Using Eqn. 2 and assuming equilibrium between the core and mantle compositions during metal segregation in a magma ocean, the FeO content of the mantle suggests an oxygen fugacity of −2.0 to −2.4 ΔIW, depending on the assumed light element composition of the Earth's core (McDonough and Sun, 1995). Gessmann and Rubie (2000) and Li and Agee (2001) applied this same constraint in their modeling studies. Applying this additional constraint, magma ocean conditions of 30–60 GPa and >2000 K are suggested. The poor constraint on temperature for this condition solution is a result of the mathematical form of the parameterizations and the partitioning behavior of Ni and Co. Since both D(Ni) and D(Co) decrease with increasing pressure, the value of C_2 for both must necessarily be negative. However, at 7 GPa, both D(Ni) and D(Co) are observed to also decrease with increasing temperature (Fig. 3). This requires that at 7 GPa, the quantity $[C_1 + C_2(P)]$ must be positive to have the partition coefficients decrease as 1/T decreases. Since C_2 has already been determined to be negative, C_1 must be positive. Thus, as the pressure increases, there will come a point when the quantity $[C_1 + C_2(P)]$ will equal zero. At this pressure, changing temperature will have no effect on the partition coefficient, leaving the temperature unconstrained in the solutions. This occurs at ~53–54 GPa for both Ni and Co, within the pressure range of the solutions at −2.2 ΔIW. At pressures higher than these, increasing temperature will cause D(Ni) and D(Co) to increase, resulting in lines with both positive and negative slopes that define the mathematically possible solution space on Figure 7.

However, in a magma ocean that does not extend all the way to the core-mantle boundary, the maximum pressure and temperature reached in the magma ocean are not independent. In this case, the base of the magma ocean will correspond to the pressure and temperature of the solidus of the mantle composition. Unfortunately, at pressures >25 GPa, the appropriate phase diagram has not been determined and a hydrous magma ocean would further affect the phase boundaries.

Additionally, the physical process of equilibrium in a magma ocean will influence the resulting siderophile element signature in the mantle. If the magma ocean is long-lived and well-mixed, ponded molten metal may equilibrate with the liquid silicate mantle at the base of the magma ocean. In this simple case, the siderophile element partitioning behavior will reflect the pressure and temperature at the base of the magma ocean. However, if the magma ocean was not well-mixed, as discussed by Li and Agee (1996, 2001), the magma ocean may have been deeper than suggested by the apparent simple metal-silicate equilibrium pressure. In recent work, Rubie et al. (2003) suggested that simple metal-silicate equilibrium at the base of a magma ocean was not likely and that metal-silicate equilibration occurred when molten metal droplets rained through the liquid silicate in the magma ocean. Modeling two extreme end-member scenarios, Rubie et al. (2003) found that the depth of the magma ocean could be either greater than or less than the depth inferred from simple metal-silicate equilibration at the base of the magma ocean by about a factor of 1.5. Thus, the implication is that the mantle concentrations of siderophile elements are still a result of the core formation process but interpreting the siderophile element signature may potentially be more complicated than simply recording a single high pressure and high temperature condition at the base of the magma ocean. Future systematic experimental studies on other moderately siderophile elements could provide further constraints on the conditions and process of terrestrial core formation in an early magma ocean.

Acknowledgments—This work was supported by NASA grants NAG5-12831 to N. L. C., 344-31-20-25 to C. B. A., and NAG5-11122 to R. P. Harvey. During early portions of this work, N. L. C. held a National Research Council NASA-JSC Research Associateship. We thank K. Righter for useful correspondences and for the use of his compiled experimental data sets. We thank T. J. McCoy and the Smithsonian Institution National Museum of Natural History for the use of their electron microprobe. We appreciate the thoughtful and thorough reviews of D. C. Rubie, M. J. Walter, and one anonymous reviewer and the comments from Associate Editor B. O. Mysen, all of which helped to greatly improve the final manuscript.

Associate editor: B. Mysen

REFERENCES

Agee C. B., Li J., Shannon M. C., and Circone S. (1995) Pressure-temperature phase diagram for the Allende meteorite. *J. Geophys. Res.* **100,** 17725–17740.

Anderson O. L. and Isaak D. G. (2002) Another look at the core density deficit of Earth's outer core. *Phys. Earth Planet. Int.* **131,** 19–27.

Asahara Y., Kubo T., and Kondo T. (2004) Phase relations of a carbonaceous chondrite at lower mantle conditions. *Phys. Earth Planet. Int.* **143–144**, 421–432.

Bouhifd M. A. and Jephcoat A. P. (2003) The effect of pressure on partitioning of Ni and Co between silicate and iron-rich metal liquids: a diamond-anvil cell study. *Earth Planet. Sci. Lett.* **209,** 245–255.

Capobianco C. J. and Amelin A. A. (1994) Metal-silicate partitioning of nickel and cobalt: The influence of temperature and oxygen fugacity. *Geochim. Cosmochim. Acta* **58,** 125–140.

Chabot N. L. and Agee C. B. (2002) The behavior of nickel and cobalt during core formation. In *Lunar and Planet. Sci. XXXIII*, Abstract #1009, Lunar and Planetary Institute, Houston (CD-ROM).

Chabot N. L. and Agee C. B. (2003) Core formation in the Earth and Moon: New experimental constraints from V, Cr and Mn. *Geochim. Cosmochim. Acta* **67,** 2077–2091.

Chabot N. L. and Jones J. H. (2003) The parameterization of solid metal-liquid metal partitioning of siderophile elements. *Meteor. Planet. Sci.* **38,** 1425–1436.

Chabot N. L., Campbell A. J., Jones J. H., Humayun M., and Agee C. B. (2003) An experimental test of Henry's Law in solid metal-liquid metal systems with implications for iron meteorites. *Meteorit. Planet. Sci.* **38,** 181–196.

Chabot N. L., Draper D. S., and Agee C. B. (2004) Core formation in the Earth: Constraints from Ni and Co. In *Workshop on Oxygen in the Terrestrial Planets*, p. 15. LPI Contribution No. 1203, Lunar and Planetary Institute, Houston.

Dingwell D. B., O'Neill H. St. C., Ertel W., and Spettel B. (1994) The solubility and oxidation state of nickel in silicate melt at low oxygen fugacities: Results using a mechanically assisted equilibration technique. *Geochim. Cosmochim. Acta* **58,** 1967–1974.

Gessmann C. K. and Rubie D. C. (1998) The effect of temperature on the partitioning of nickel, cobalt, manganese, chromium and vanadium at 9 GPa and constraints on formation of the Earth's core. *Geochim. Cosmochim. Acta* **62,** 867–882.

Gessmann C. K. and Rubie D. C. (2000) The origin of the depletions of V, Cr and Mn in the mantles of the Earth and Moon. *Earth Planet. Sci. Lett.* **184,** 95–107.

Hillgren V. J., Drake M. J., and Rubie D. C. (1994) High pressure and high temperature experiments on core-mantle segregation in the accreting Earth. *Science* **264,** 1442–1445.

Hillgren V. J., Drake M. J., and Rubie D. C. (1996) High pressure and high temperature metal-silicate partitioning of siderophile elements: The importance of silicate liquid composition. *Geochim. Cosmochim. Acta* **60,** 2257–2263.

Hillgren V. J., Gessmann C. K., and Li J. (2000) An experimental perspective on the light element in Earth's core. In *Origin of the Earth and Moon* (eds. R. M. Canup and K. Righter), pp. 245–263. The University of Arizona Press, Tucson.

Holzheid A., Borisov A., and Palme H. (1994) The effect of oxygen fugacity and temperature on solubilities of nickel, cobalt and molybdenum in silicate melts. *Geochim. Cosmochim. Acta* **58,** 1975–1981.

Holzheid A. and Palme H. (1996) The influence of FeO on the solubilities of cobalt and nickel in silicate melts. *Geochim. Cosmochim. Acta* **60,** 1181–1193.

Ito E., Katsura T. and Suzuki T. (1998) Metal/silicate partitioning of Mn, Co and Ni at high-pressures and high temperatures and implications for core formation in a deep magma ocean. In *Properties of Earth and Planetary Materials at High Pressure and Temperature* (eds. M. H. Manghnani and T. Yagi) *Geophysical Monograph* **101**, 215–225.

Jaeger W. L. and Drake M. J. (2000) Metal-silicate partitioning of Co, Ga and W: Dependence on silicate melt composition. *Geochim. Cosmochim. Acta* **64,** 3887–3895.

Jana D. and Walker D. (1997a) The impact of carbon on element distribution during core formation. *Geochim. Cosmochim. Acta* **61,** 2759–2763.

Jana D. and Walker D. (1997b) The influence of silicate melt composition on distribution of siderophile elements among metal and silicate liquids. *Earth Planet. Sci. Lett.* **150,** 463–472.

Jana D. and Walker D. (1997c) The influence of sulfur on partitioning of siderophile elements. *Geochim. Cosmochim. Acta* **61,** 5255–5277.

Jones J. H. and Drake M. J. (1983) Experimental investigations of trace element fractionation in iron meteorites, II: The influence of sulfur. *Geochim. Cosmochim. Acta* **47,** 1199–1209.

Jones J. H. (1998) Uncertainties in modeling core formation. *Meteorit. Planet. Sci.* **33,** A79–80.

Kegler Ph., Holzheid A., Rubie D. C., Frost D. and Palme H. (2004) Reinvestigation of the Ni and Co metal-silicate partitioning. In *Lunar and Planet. Sci. XXXV*, Abstract #1632, Lunar and Planetary Institute, Houston (CD-ROM).

Kilburn M. R. and Wood B. J. (1997) Metal-silicate partitioning and the incompatibility of S and Si during core formation. *Earth Planet. Sci. Lett.* **152,** 139–148.

Lauer H. V. and Jones J. H. (1999) Tungsten and Nickel partitioning between solid and liquid metal; implications for high-pressure metal/silicate experiments. In *Lunar and Planet. Sci. XXX*, Abstract #1617, Lunar and Planetary Institute, Houston (CD-ROM).

Lewis R. D. and Lofgren G. E. (1991) The effect of sodium vapor on the sodium content of chondrules. *Proc. Lunar and Planet. Sci. Conf.* **XXII**, 805–806.

Li J. and Agee C. B. (1996) Geochemistry of mantle-core differentiation at high pressure. *Nature* **381,** 686–689.

Li J. and Agee C. B. (2001) The effect of pressure, temperature, oxygen fugacity and composition on partitioning of nickel and cobalt between liquid Fe-Ni-S alloy and liquid silicate: Implications for the Earth's core formation. *Geochim. Cosmochim. Acta* **65,** 1821–1832.

McDonough W. F. and Sun S.-s. (1995) The composition of the Earth. *Chem. Geol.* **120,** 223–253.

Okamoto H. (1990) C-Fe (Carbon-Iron). In *Binary Alloy Phase Diagrams* (ed. T. B. Massalski) Vol. 1pp. 842–848. ASM International, USA.

Ohtani E., Yurimoto H., and Seto S. (1997) Element partitioning between metallic liquid, silicate liquid and lower-mantle minerals: implications for core formation of the Earth. *Phys. Earth Planet. Int.* **100,** 97–114.

Righter K., Drake M. J., and Yaxley G. (1997) Prediction of siderophile element metal/silicate partition coefficients to 20 *GPa and 2800°C: the effects of pressure, temperature, oxygen fugacity and silicate and metallic melt compositions. Phys. Earth Planet. Int.* **100,** 115–134.

Righter K. and Drake M. J. (1999) Effect of water on metal-silicate partitioning of siderophile elements: a high pressure and temperature terrestrial magma ocean and core formation. *Earth Planet. Sci. Lett.* **171,** 383–399.

Righter K. and Drake M. J. (2001) Constraints on the depth of an early terrestrial magma ocean. *Meteorit. Planet. Sci.* **36,** A. 173.

Ringwood A. E. (1966) The chemical composition and origin of the Earth. In *Advances in Earth Science* (ed. P. Hurley), pp. 357–398. MIT Press, Boston, MA, USA.

Rubie D. C., Melosh H. J., Reid J. E., Liebske C., and Righter K. (2003) Mechanisms of metal-silicate equilibration in the terrestrial magma ocean. *Earth Planet. Sci. Lett.* **205,** 239–255.

Thibault Y. and Walter M. J. (1995) The influence of pressure and temperature on the metal-silicate partition coefficients of nickel and cobalt in a model C1 chondrite and implications for metal segregation in a deep magma ocean. *Geochim. Cosmochim. Acta* **59,** 991–1002.

Walter M. J., Newsom H. E., Ertel W., and Holzheid A. (2000) Siderophile elements in the Earth and Moon: Metal/silicate partitioning and implications for core formation. In *Origin of the Earth and Moon* (eds. R. M. Canup, K. Righter) pp. 265–289. The University of Arizona Press, Tucson.

Wänke H. (1981) Constitution of terrestrial planets. *Phil. Trans. R. Soc. Lond. A* **303,** 287–302.

Wood B. J. (1993) Carbon in the core. *Earth Planet. Sci. Lett.* **117,** 593–607.

Zhang J. and Herzberg C. (1994) melting experiments on anhydrous peridotite KLB-1 from 5.0 to 22.5 GPa. *J. Geophys. Res.* **99,** 17729–17742.